analytical chemistry

Article

pubs.acs.org/ac

Stepwise Chemical Reaction Strategy for Highly Sensitive Electrochemiluminescent Detection of Dopamine

Lei Zhang, Yan Cheng, Jianping Lei,* Yueting Liu, Qing Hao, and Huangxian Ju

State Key Laboratory of Analytical Chemistry for Life Science, School of Chemistry and Chemical Engineering, Nanjing University, Nanjing 210093, P. R. China

Supporting Information

ABSTRACT: A stepwise chemical reaction strategy based on the specific recognition of boronic acid to diol, and *N*-hydroxysuccinimide (NHS) ester to amine group, was designed to construct a "signal on" electrochemiluminescence (ECL) platform for highly sensitive detection of dopamine. A boronic acid-functionalized pyrene probe was synthesized and was self-assembled on the sidewalls of carbon nanotubes via $\pi-\pi$ stacking interactions as capture probes on a glassy carbon electrode. Meanwhile, 3,3′-dithiodipropionic acid di(*N*-hydroxysuccinimide ester) (DSP)-functionalized CdTe quantum dots (QDs) were designed as signal probes and characterized with transmission electron microscopy and spectroscopic techniques. Upon stepwise chemical reaction of dopamine with boronic acid and then DSP-QDs, the QDs were captured on the electrode as ECL emitters for signal readout, leading to an ultralow background signal. By using O_2 as an endogenous coreactant, the "signal on" ECL method was employed to quantify the concentration of dopamine from 50 pM to 10 nM with a detection limit of 26 pM. Moreover, the stepwise chemical reaction-based biosensor showed high specificity against cerebral interference and was successfully applied in the detection of dopamine in cerebrospinal fluid samples. The stepwise chemical reaction strategy should be a new concept for the design of highly selective analytical methods for the detection of small biomolecules.

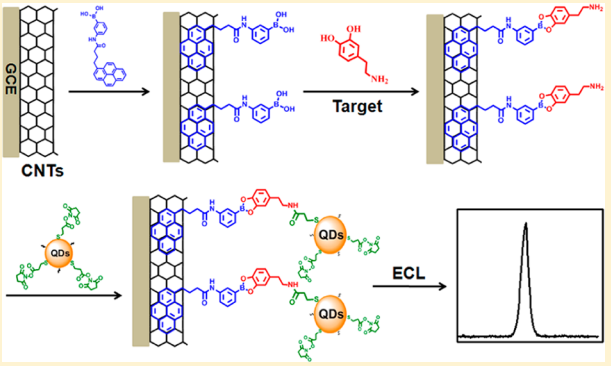

Electrochemiluminescence (ECL) as a sensitive technique has attracted continuous interest owing to the integrated advantages of electrochemistry and chemiluminescence.[1] Especially, semiconductor quantum dot (QD)-based ECL has been widely applied in bioanalysis because QDs own several unique merits such as size-controlled luminescence and good stability against photobleaching.[2−4] QD-based ECL biosensing strategies are usually divided into four methodologies: the inhibition/enhancement effect of the analyte, generation/consumption of coreactant, steric hindrance from the biorecognition reaction, and ECL resonance energy transfer.[5] Because QDs in these strategies are immobilized directly on the electrode surface as a sensing element, QD-based ECL analytical methods suffer from a high background, which precludes their application in practice. To reduce the background, it is preferred to introduce labeled QDs to the electrode via molecular recognition for signal readout.[6] In fact, many ECL detection methods using QDs as detection probes have been developed via biomacromolecular recognition such as antibody−antigen and aptamer−protein.[7−11] However, ECL sensing of small biomolecules is still a great challenge due to the lack of specific recognition sites. Therefore, it was desirable to seek a new binding approach to enhance specificity in the QD-based ECL detection of small biomolecules.

Fortunately, this issue can be addressed through a stepwise chemical or biological recognition strategy, in which a molecule is sequentially recognized by other molecules at different sites to improve specificity. A stepwise molecular recognition strategy has been applied in the preparation of supramolecular structures, sandwich immunoassays, and chiral sensing.[12−17] For example, by using a dual recognition linker, β-cyclodextrin/α-mannopyranoside, which can act as a host for chemical molecular recognition of the adamantane and as a ligand for biological recognition of concanavalin A simultaneously, self-assembled protein−polymer conjugates were attained.[12] On the basis of target versatility (amines and diols) with ferrocene-based chiral boronic acids, a chiral sensor was constructed for the determination of enantiomeric excess of binol by using an electrochemical method.[13] The method based on stepwise chemical reaction was especially favorable for selective detection of small molecules due to the sequential recognition processes. Here, on the basis of stepwise chemical reaction between a boronic acid and a diol, and an amine group and *N*-hydroxysuccinimide (NHS) ester, an ECL biosensor was designed for highly sensitive and selective detection of dopamine.

Received: June 24, 2013
Accepted: July 31, 2013
Published: July 31, 2013

   dx.doi.org/10.1021/ac401894w | *Anal. Chem.* 2013, 85, 8001−8007

Scheme 1. (A) Synthesis of the Recognition Probe, (B) the Functionalization of QDs with DSP, and (C) the Stepwise Chemical Reaction Strategy for ECL Detection of Dopamine

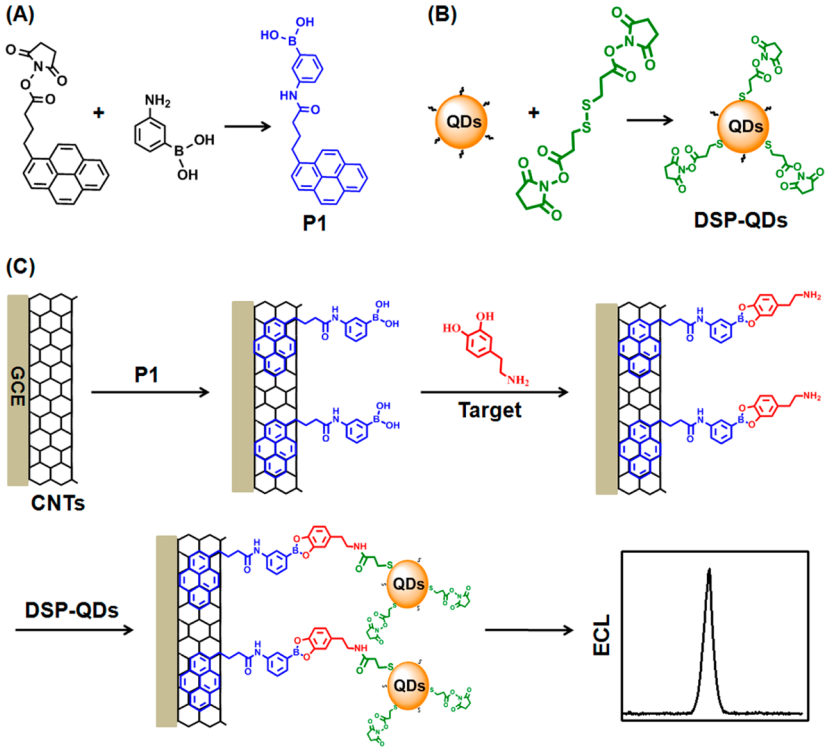

Dopamine (DA) as an important neurotransmitter plays a very important role in the renal, hormonal, and cardiovascular systems, and abnormal levels of DA are related to neurological disorders such as Parkinson's disease.[18] Many elegant methods have been reported for DA determination, including chromatography combined with mass spectrometry,[19] UV−vis spectrophotometry,[20] fluorometry,[21] and electrochemical techniques.[22,23] Although those methods for the detection of dopamine can reach a low detection limit, most of them suffer from low selectivity in the presence of other catechol derivatives. Meanwhile, a single molecular recognition method was also imperfect in terms of specificity. In the case of ECL detection of DA, ECL was conventionally quenched by the oxidation products of DA and charge/energy-transfer between the analytes and ECL emitters on the electrode.[24−29] In this work, by using labeled QDs as signal probes, a "signal on" ECL detection strategy was proposed by coupling with stepwise chemical reaction for selective and sensitive detection of DA (Scheme 1). First, a boronic acid-functionalized pyrene probe (**P1**) was synthesized, which was self-assembled on the sidewalls of carbon nanotubes (CNTs) via $\pi-\pi$ stacking interactions as a capture probe on a glassy carbon electrode (GCE). Then the immobilized **P1** would recognize DA via specific interaction between boronic acid and diol. Sequentially, 3,3′-dithiodipropionic acid di(*N*-hydroxysuccinimide ester) (DSP)-functionalized CdTe QDs were covalently bound with DA via amidation. Therefore, the QDs were captured on the electrode as ECL emitters, and then the "signal on" ECL emission was observed by using O_2 as an endogenous coreactant. The proposed method shows a detection limit down to picomoles and high selectivity for the determination of DA in real samples. This work is the first report on the "signal on" ECL sensor for the detection of DA based on stepwise chemical reaction and extends the applications of ECL in the selective detection of small biomolecules.

EXPERIMENTAL SECTION

Materials and Reagents. Cadmium chloride ($CdCl_2 \cdot 2.5H_2O$), *meso*-2,3-dimercaptosuccinic acid (DMSA), and dopamine hydrochloride were purchased from Alfa Aesar China Ltd. Uric acid (UA), D-(+)-glucose, lactate, 3,4-dihydroxyphenylacetic acid (DOPAC), homovanillic acid (HVA), epinephrine hydrochloride, catechol, L-tyrosine, and glutamic acid were purchased from Shanghai J&K Chemical Ltd. (China). 3-Aminophenylboronic acid, 1-pyrenebutanoic acid succinimidyl ester, and 3,3′-dithiodipropionic acid di(*N*-hydroxysuccinimide ester) were purchased from Sigma-Aldrich and used as supplied. L-Ascorbic acid (AA) was purchased from Sinopharm Chemical Reagent Co., Ltd. Noradrenaline bitartrate was purchased from Chengdu Xiya Chemical Technology Co., Ltd. Carbon nanotubes (CNTs, CVD method, purity 98%, multiwalled, diameter 40−60 nm, and length 1−2 μm) were purchased from Shenzhen Nanotech Port Co., Ltd. (Shenzhen, China). Phosphate buffer (PBS) (0.1 M, pH 9.0) was prepared by mixing stock solutions of NaH_2PO_4 and Na_2HPO_4 with 0.1 M KNO_3 as the supporting electrolyte. Other reagents were of analytical grade and used as received. Ultrapure water (≥18 MΩ, Milli-Q, Millipore) was used throughout the work.

Multiwalled CNTs were first sonicated with 3:1 (v/v) H_2SO_4/HNO_3 for 4 h to obtain carboxylic group-functionalized CNTs. The resulting dispersion was filtered and washed repeatedly with water until the pH was about 7.0. The collected functionalized CNTs were redispersed in water to a concentration of 0.1 mg mL^{-1}.

For the determination of DA in practice, two real cerebrospinal fluid (CSF) samples were kindly obtained from

dx.doi.org/10.1021/ac401894w | *Anal. Chem.* 2013, 85, 8001−8007

volunteer patients. Before utilization, CSF samples were centrifuged at 14 000 rcf for 15 min and the supernates were collected. After precipitation of the proteins in the samples by acetonitrile, the resulting supernates were further centrifuged at 12 000 rcf for 15 min to get the final samples for assay.

Apparatus. X-ray photoelectron spectroscopy (XPS) experiments were carried out on an ESCALAB 250 spectrometer (Thermo-VG Scientific Co., Waltham, MA) with an ultrahigh vacuum generator. Infrared (IR) spectra were recorded on a Nicolet NEXUS870 Fourier transform infrared (FT-IR) spectrometer (Madison, WI). The UV−vis absorption spectra were obtained with a UV-3600 UV−vis-NIR spectrophotometer (Shimadzu Co., Kyoto, Japan). The transmission electron micrograph (TEM) was obtained using a JEM-2100 TEM instrument (JEOL, Japan). ESI-MS was recorded on an Agilent G6540Q-TOF LC/MS equipped with an electrospray ionization (ESI) probe operating in positive ion mode. ^{1}H and ^{13}C NMR spectra were recorded on a Bruker APX-400 spectrometer with chemical shifts referenced to $SiMe_4$ as internal standard. Electrochemical impedance spectroscopic (EIS) measurements were carried out on a PGSTAT30/FRA2 system (Autolab, The Netherlands) in 0.1 M KCl containing 5 mM $K_3Fe(CN)_6/K_4Fe(CN)_6$. Electrochemiluminescent measurements were carried out on a MPI-E multifunctional electrochemical and chemiluminescent analytical system (Xi'an, China), with a modified glassy carbon electrode (GCE, 5 mm in diameter, China) as a working, a platinum wire as a counter, and a Ag/AgCl (saturated KCl) as a reference electrode. The ECL emission window was placed in front of the photomultiplier tube (PMT, detection range from 300 to 650 nm) biased at 1000 V with scan rate of 100 mV/s.

Synthesis of P1. A mixture of 3-aminophenylboronic acid (30.9 mg, 0.2 mmol) and 1-pyrenebutanoic acid succinimidyl ester (77.1 mg, 0.2 mmol) in methanol (10 mL) was sonicated for 2 h. The crude product was directly purified by flash chromatography in 1/1 (v/v) ethyl acetate/petroleum ether to afford the product as a pale yellow solid. Yield: 21.3 mg, 26.4%. ESI-MS: m/z 440.42, $[M + CH_3OH + H]^+$. ^{1}H NMR (400 MHz, C_6D_6): δ (ppm) 8.49 (s, 1H), 8.17−7.66 (m, 13H), 3.26 (s, 2H), 3.11 (t, J = 7.6 Hz, 2H), 2.35 (t, J = 6.8 Hz, 2H), 2.0−1.94 (m, 2H). ^{13}C NMR (400 MHz, DMSO-d_6): δ (ppm) 172.3, 171.1, 135.9, 130.8, 130.4, 130.3, 129.6, 129.4, 128.1, 128.0, 127.5, 127.4, 127.3, 126.5, 126.1, 126.0, 125.0, 124.9, 124.8, 124.2, 124.1, 123.4, 123.3, 31.6, 30.7, 26.7 (Figures S1−S3 in Supporting Information).

Synthesis of QDs and DSP-QDs. The DMSA-stabilized CdTe (DMSA-CdTe) QDs were prepared according to the reported electrolysis method.[30] Briefly, 7.8 mg of DMSA was dissolved by stirring in 20 mL of ultrapure water. After regulation of the pH to around 9.0, 120 μL of 0.1 M $CdCl_2$ was next added dropwise to obtain a homogeneous solution. When a terminal charge quantity of 0.5 °C was reached upon the applied potential of about −1.0 V at a polished tellurium electrode, the resulting solution was air-proofed and immersed in a constant temperature bath at 80 °C for 20 h to harvest DMSA-CdTe QDs and then stored at 4 °C in the dark. Before usage, the as-prepared QD solution was purified, sedimented in 1:1 (v/v) isopropyl alcohol/water, and centrifuged at 8000 rcf for 5 min. The precipitate was then dissolved in deionized water.

DSP-QDs were prepared by mixing 0.50 mL of the redissolved QDs with 0.45 mL of 2 mM DSP via ligand exchange. The mixture was allowed to react ultrasonically under low modulated frequency for over 0.5 h and then incubated for 4−6 h at room temperature. Successively, the unreacted DSP was removed from the DSP-QDs by filtration in a Millipore Microcon (10 000 MW) at 8000 rcf for 8 min. The product was washed with acetone twice. The final product was redissolved in deionized water and stored at 4 °C in the dark prior to use.

Construction of the ECL Biosensor. The GCE was polished successively with 1.0, 0.3, and 0.05 mm of alumina slurry (Beuhler). After successive sonication in ethanol and deionized water, the electrode was dried under N_2. To accelerate electron transfer and provide a large surface for immobilization of **P1**, 10 μL of a 0.1 mg mL^{-1} multiwalled CNT dispersion was spread on a pretreated bare GCE and dried at room temperature. Ten microliters of 0.5 mmol L^{-1} **P1** solution was then dropped onto the CNT film. After removal of excess **P1** with water, 10 μL of the appropriate concentration of DA solution was applied to the CNT−**P1** layer in the dark for 3 h. The resulting surface was incubated with 10 μL of DSP-QDs for 4 h after washing with deionized water to remove the unreacted DA. The whole assay time including the construction of the biosensor was around 7 h. Finally, the as-prepared biosensor was rinsed three times with deionized water to eliminate the noncovalently absorbed DSP-QDs, and then ECL measurements for signal readout were carried out by using dissolved O_2, without introduction of exogenous coreactants such as $S_2O_8^{2-}$, which was beneficial to the biosensor.

RESULTS AND DISCUSSION

Characterization of DSP-QDs. The UV−vis spectrum of QDs showed a wide absorption band with an absorption inflection point at 460 nm that is consistent with the data described previously (Figure 1A, curve a).[31] After modification

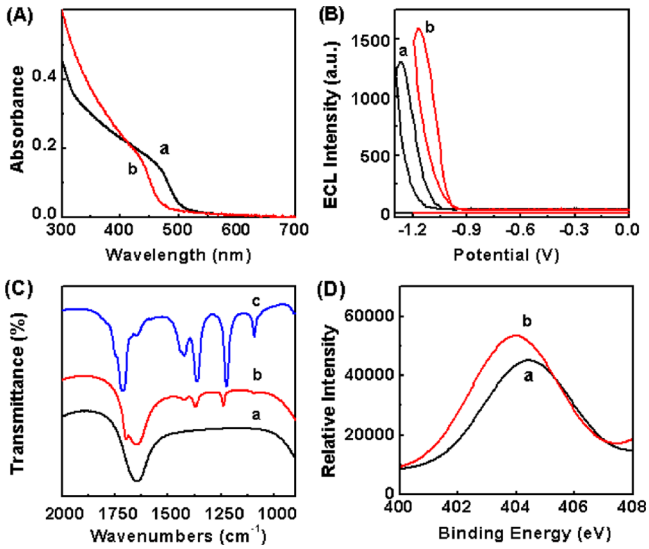

Figure 1. (A) UV−vis absorption spectra. (B) ECL emission curves with PMT biased at 900 V. (C) FT-IR spectra and (D) Cd3d XPS of QDs (a) and DSP-QDs (b). Curve c is the FT-IR spectrum of DSP.

with DSP, the absorption peak of DSP-QDs significantly blue-shifted to 437 nm (Figure 1A, curve b), which indentified that DSP was assembled on the surface of QDs. According to Peng's empirical equation, the concentration of the redispersed DSP-QD solution was estimated to be ~23 μM.[32] The ECL emission peak of DSP-QDs occurred at a potential more positive than that of QDs (Figure 1B), suggesting surface-state ECL emission

dx.doi.org/10.1021/ac401894w | Anal. Chem. 2013, 85, 8001−8007

in this designed system.[33] The IR spectra also confirmed that the ligand of DSP was successfully linked with QDs (Figure 1C). Compared with QDs (curve a), DSP-QDs showed the characteristic vibrational frequencies of DSP at 1710.6, 1421.7, 1363.2, 1235.3, and 1095.0 cm^{-1} corresponding to C═O stretching vibration, two C−H bending vibrations of methylene, C−O asymmetric stretching vibration, and C−O symmetric stretching vibration, respectively (curve b). DSP-QDs were as well validated from XPS by the alteration of the binding energy (Figure 1D). It displayed a mild movement of the Cd 3d peak from 404.2 to 403.9 eV in which Cd 3d somewhat coincided with N1s (402.9 ev) of DSP. In other words, these results successfully verified the assembly of DSP to the surface of QDs.

Characterization of Stepwise Assembly of ECL Biosensor. TEM images showed the morphology change during the construction of the sensor. First, the TEM image of the acid-pretreated CNTs displayed a uniform structure in the form of single tubes or small bundles with diameters of 40−60 nm (Figure 2A). The size of the DSP-QDs was estimated to be

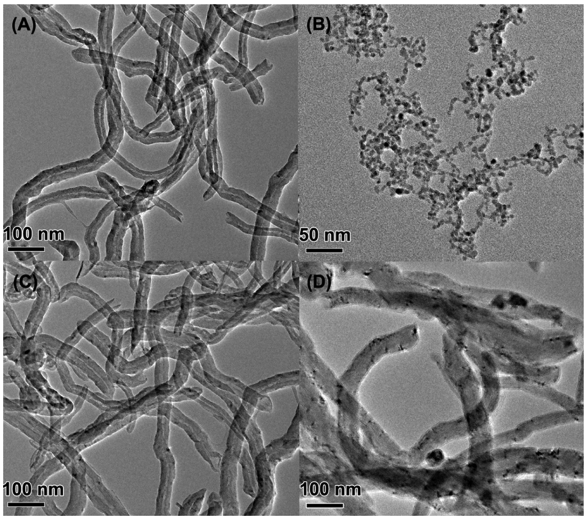

Figure 2. TEM images of (A) CNTs, (B) DSP-QDs, (C) CNTs/**P1**/DA, and (D) CNTs/**P1**/DA/DSP-QDs.

4.0−6.5 nm by TEM (Figure 2B). When **P1** was assembled on the surface of CNTs, no obvious change was observed compared with that of pure CNTs (Figure 2C). Sequentially, DSP-QDs were assembled on the CNTs, and many black dots appeared on the CNTs (Figure 2D), which became blurry with the increase in their average diameter, indicating successful assembly of the DSP-QDs on the biosensor surface. Furthermore, DSP-QDs appeared only on the surface of CNTs, suggesting specific recognition in the ECL detection. These results suggested that the designed ECL platform has the capacity for sensitive detection with an ultralow background.

On the other hand, electrochemical impedance spectra were utilized to monitor the sequential fabrication of the ECL sensor (Figure 3A). The bare GCE showed a relatively small electron-transfer resistance (R_{et}) (curve a). After CNTs were immobilized on the electrode, R_{et} decreased (curve b), indicating that the high electrical conductivity of the CNTs facilitated the electron transfer. The modification of the CNTs with **P1** by $\pi-\pi$ stacking led to a much larger R_{et} (curve c) because it blocked the electron transfer in the CNTs. Finally, the presence of QDs greatly enhanced the R_{et} (curve e) due to the unique properties of this semiconductor.[34] The impedances of the biosensor in the absence and presence of DA were similar (curves c and d), indicating that the binding of DA as a small organic molecule did not greatly affect the electron transfer. On the whole, the tendency for increased impedances further testified to the immobilization of these substances on the electrode surface.

Feasibility of the ECL Biosensor. In the present sensor, DSP-QDs as a signal probe were finally introduced to the electrode by covalent reaction with DA instead of direct physical absorption as in most ECL detections. IR spectra were employed to prove the successful covalent linkage between DSP-QDs and DA (Figure 3B). After the reaction of DSP-QDs with DA, the peaks at 3009.9, 2976.6, 2931.4, and 950.1 cm^{-1} disappeared, which correspond to three stretching vibrations of C−H, and one stretching vibration of N−O in the NHS group of DSP, respectively, because NHS esters as a good leaving group can react with amine via amidation. Meanwhile, the stretching vibration around 1650 cm^{-1} was significantly enhanced due to the formation of amide I via reaction between the amine group of DA and the NHS ester of DSP-QDs.

The feasibility of the ECL biosensor was further investigated by measuring the ECL signal in the presence or absence of the target (Figure 4). In the absence of the target, no ECL signal was observed at the constructed sensor (curve a) because no DSP-QDs were absorbed on the electrode after rinsing with water. In contrast, in the presence of the target, a sharp ECL emission peak appeared at −1.16 V (curve b). To exclude that the ECL signal was caused by the nonspecific absorption of

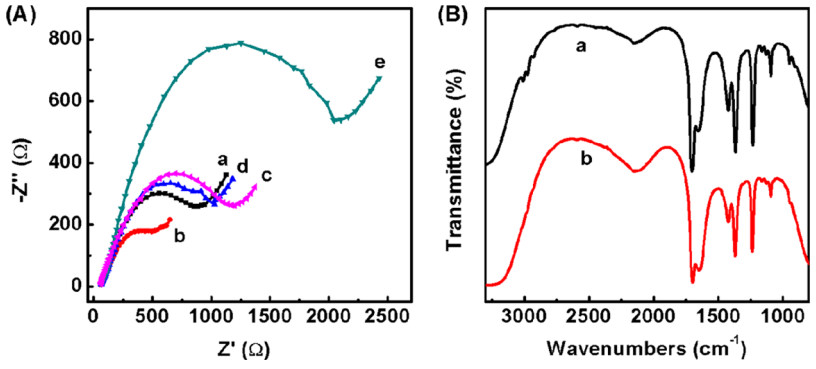

Figure 3. (A) EIS plots of bare GCE (a), GCE/CNTs (b), GCE/CNTs/**P1** (c), GCE/CNTs/**P1**/DA (d), and GCE/CNTs/**P1**/DA/DSP-QDs (e). (B) FT-IR spectra of DSP-QDs (a) and DSP-QDs/DA (b).

dx.doi.org/10.1021/ac401894w | *Anal. Chem.* 2013, 85, 8001−8007

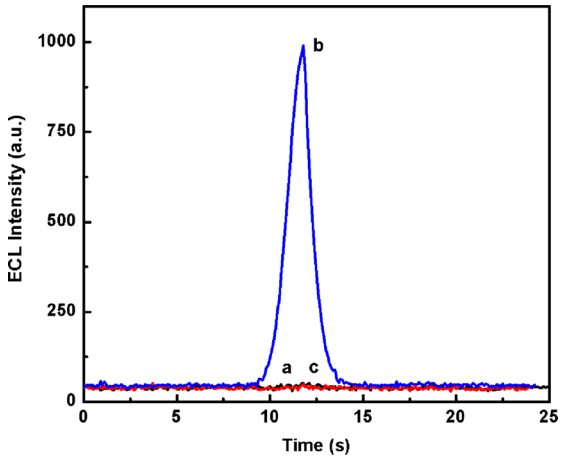

Figure 4. ECL responses of the GCE/CNTs/**P1** in air-saturated 0.1 M pH 9.0 PBS in the presence of DSP-QDs (a), DA + DSP-QDs (b), and DA + DMSA-QDs (c).

QDs, the response of the sensor was investigated in the presence of DA by using no DSP-functionalized QDs as a signal probe. As shown in curve c, no obvious ECL peak was observed. Therefore, a highly sensitive strategy for "signal on" ECL sensing of DA was developed by stepwise chemical reaction between boronic acid and diol, and then between the amine group and NHS ester, among the **P1**, DA, and DSP-QDs. Moreover, the proposed method of QD immobilization on GCE by stepwise chemical reaction greatly decreased the background for highly sensitive detection.

Optimization of Detection Conditions. The pH of the electrolyte is a significant factor relevant to the ECL response. To obtain sufficient ECL intensity, the influence of the detection solution pH on the ECL response of DSP-QDs was investigated as shown in Figure 5A. In the examined pH range, the ECL intensity increased as the pH changed from 6.0 to 9.0 because the electrogenerated intermediates (e.g., $O_2^{\bullet-}$ and $HO^{\bullet}$) of dissolved O_2 as well as the resulting H_2O_2 as the coreactant were more stable at high pH. Taking into account further application under physiological conditions, pH 9.0 PBS was used as the detection solution.

The incubation time is another important parameter that influences the ECL signal (Figure 5B). At room temperature, the ECL signal was enhanced as the incubation time increased and then approached a constant value after 4 h (curve b), which was limited by the saturated binding site between DA and DSP-QDs. Conversely, no obvious signal change was observed for DSP-QDs in the absence of DA (curve a). Therefore, 4 h of incubation time was selected for the ECL biosensor.

ECL Response to DA. Under optimal conditions, the stepwise chemical reaction strategy was performed by the reaction of DA at a known concentration with **P1** as the recognition probe and then with DSP-QDs as the signal probe. The captured DSP-QDs on the sensor surface gave ECL emission at the applied potential to produce a detectable signal at different electrodes for different concentrations of the target. As shown in Figure 6A, the ECL signal increased as the concentration of DA increased. The calibration plot shows a good linear relationship between the ECL intensity and the logarithmic value of DA concentration in a range of 50 pM to 10 nM (inset in Figure 6A). The regression equation was $I = 2872.3 + 257.5 \times \log c$ with a correlation coefficient of 0.992, where I is the ECL intensity of the biosensor in the presence of DA, and c is the concentration of DA. The detection limit at a signal-to-noise ratio of 3 was 26 pM, which was much lower than 0.1 μM of the near-infrared Ag_2Se QD-based ECL method,[26] 30 nM of the graphene oxide-based electrochemical method,[35] and 50 nM of the mesoporous silica particle-based fluorescent sensing method.[36] The low detection limit of the proposed biosensor is attributed to the ultralow background signal resulting from dual molecular recognition and the "signal on" detection strategy.

Selectivity of the ECL Biosensor. Selective electrochemical determination of DA is usually limited by the lack of the resolution between DA and other electroactive compounds coexisting in cerebral systems, because they can be electrochemically oxidized at similar potentials.[37−39] In the proposed ECL sensor, a high selectivity for DA was achieved by a stepwise chemical reaction strategy, which was required both for boronic acid recognition of the catechol group of DA, and for DSP recognition of amine group of DA. Therefore, possible interference from physiological components, such as glucose, 3,4-dihydroxyphenylacetic acid, tyrosine, ascorbic acid, catechol, uric acid, homovanillic acid, lactate, glutamic acid, and the catecholamines epinephrine and norepinephrine, were examined (Figure 7A). Although norepinephrine has reactive groups similar to that of DA, further reaction may be blocked by steric hindrance from the hydroxyl group near the amine group. Thus, no obvious response was observed in the present biosensor, indicating excellent selectivity of the designed biosensor. Moreover, the antiinterference experiment was performed by measuring a solution containing 2 nM DA and

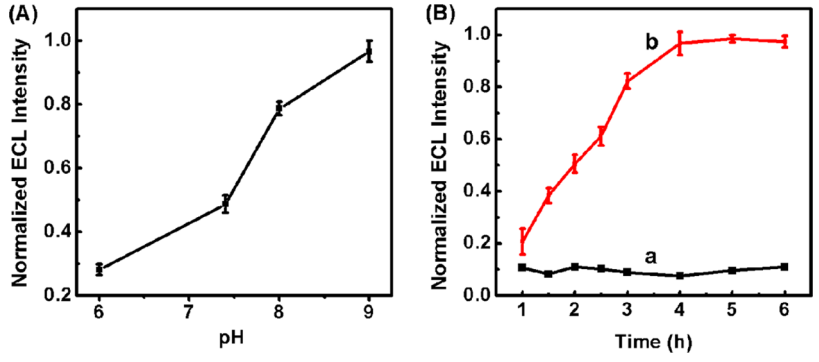

Figure 5. Effects of (A) pH of detection solution and (B) incubation time of DSP-QDs in the absence (a) and presence (b) of 10 nM DA on the ECL response. When one parameter is changed, the others are at their optimal value.

dx.doi.org/10.1021/ac401894w | *Anal. Chem.* 2013, 85, 8001−8007

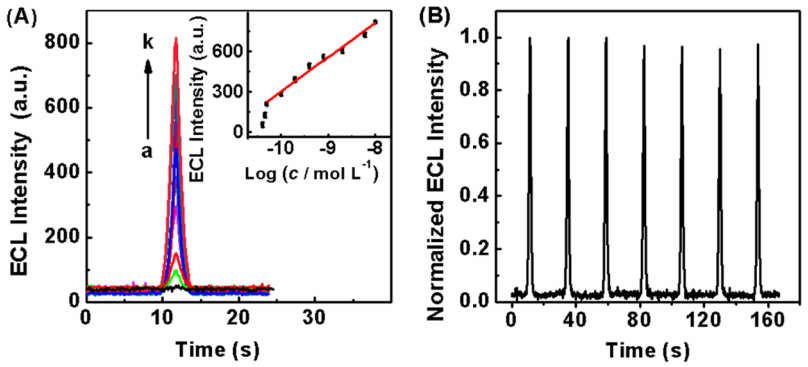

Figure 6. (A) ECL responses of the optimized sensor to different concentrations of DA: 0, 0.04, 0.045, 0.05, 0.1, 0.2, 0.4, 0.8, 2, 6, and 10 nM (from a to k). Inset: plot of ECL intensity vs logarithmic value of DA concentration. (B) Continuous cyclic scans at GCE/CNTs/**P1**/DA/DSP-QDs in the air-saturated detection solution.

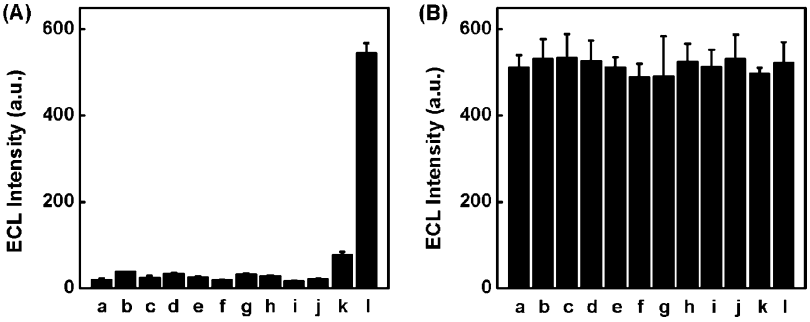

Figure 7. ECL responses of the biosensor toward 10 nM glutamic acid, glucose, 3,4-dihydroxyphenylacetic acid, tyrosine, ascorbic acid, catechol, uric acid, homovanillic acid, lactate, epinephrine, and norepinephrine (from a to k) in the absence (A) and in the presence (B) of 2 nM DA. Column l is ECL response of the sensor toward 2 nM DA.

10 nM interfering reagent as listed above. Similarly, no obvious change was observed (Figure 7B), indicating acceptable selectivity for DA detection.

Reproducibility and Precision of the ECL Biosensor. The interassay precision of five ECL sensors was examined at 1.0 nM DA. The relative standard deviation (RSD) of the five measurements was 4.7%, showing good precision and acceptable fabrication reproducibility. Seven measurements of ECL emission from continuous cyclic scans of the ECL sensor at 1.0 nM DA showed a coincident signal with an RSD of 1.7% (Figure 6B), indicating acceptable reliability and stability of the detection signal. The stability of the sensor for DA was also examined by measuring the ECL responses after storage at 4 °C for 10 days. The ECL response had no obvious decline with an RSD of 7.6%, demonstrating good stability of the sensor.

Application in Cerebrospinal Fluid Samples. To evaluate the applicability and reliability of the present ECL system, two real cerebrospinal fluid (CSF) samples were examined (Table 1). Due to low concentrations of DA in the CSF of patients, the low detection limit at the picomolar level in the present report was especially appropriate for the analysis of the CSF samples. After pretreatment, the DA concentrations in the samples were 39.8 and 60 pM by the standard addition method, which is consistent with the value reported in ref 40. The average recoveries ranged from 101.9% ± 6.9% to 107.7% ± 3.6% for three determinations, indicating good accuracy and acceptable precision. Thus, the present method is satisfactory for practical application in the detection of DA for clinical diagnosis.

Table 1. Detection Results and Recoveries of DA in CSF Samples

sample no.	addition, pM	found, pM	recovery, %
1	0	39.8	
	24	66.7	104.6 ± 4.8
	48	89.5	101.9 ± 6.9
2	0	60.0	
	30	96.9	107.7 ± 3.6
	60	124.4	103.7 ± 6.0

CONCLUSIONS

A universal electrochemiluminescent platform was designed with a stepwise chemical reaction strategy for the highly sensitive detection of small biomolecules. Because it required two chemical recognitions, both boronic acid−diol and NHS ester−amine, the present approach showed excellent selectivity for the target. Moreover, compared with the direct physical absorption of QDs in conventional ECL methods, the present approach captured the QDs as a signal probe to the electrode by covalent chemical reaction. Therefore, the "signal on" ECL sensing strategy was achieved and further decreased the background to allow for highly sensitive detection of DA. By using O_2 as an endogenous coreactant for the ECL signal output, this biosensor showed wide linear response range, low detection limit in the picomole range, and extremely high selectivity for DA and was successfully applied for the detection of dopamine in real samples. This stepwise chemical reaction strategy provides a powerful tool to design biosensing

dx.doi.org/10.1021/ac401894w | *Anal. Chem.* 2013, 85, 8001−8007

approaches for the highly selective detection of small biomolecules.

■ ASSOCIATED CONTENT

Supporting Information

Additional information as noted in text. This material is available free of charge via the Internet at http://pubs.acs.org.

■ AUTHOR INFORMATION

Corresponding Author

*Phone/Fax: +86-25-83593593. E-mail: jpl@nju.edu.cn.

Notes

The authors declare no competing financial interest.

■ ACKNOWLEDGMENTS

This work was financially supported by the National Basic Research Program of China (2010CB732400), National Natural Science Foundation of China (21075060, 21135002, 21121091), and the program for New Century Excellent Talents in University (NCET100479).

■ REFERENCES

(1) Richter, M. M. *Chem. Rev.* **2004**, *104*, 3003−3036.
(2) Bruchez, M.; Moronne, M.; Gin, P.; Weiss, S.; Alivisatos, A. P. *Science* **1998**, *281*, 2013−2016.
(3) Chan, W. C. W.; Nie, S. M. *Science* **1998**, *281*, 2016−2018.
(4) Michalet, X.; Pinaud, F. F.; Bentolila, L. A.; Tsay, J. M.; Doose, S.; Li, J. J.; Sundarensan, G.; Wu, A. M.; Gambhir, S. S.; Weiss, S. *Science* **2005**, *307*, 538−544.
(5) Deng, S. Y.; Ju, H. X. *Analyst* **2013**, *138*, 43−61.
(6) Yuan, L.; Hua, X.; Wu, Y. F.; Pan, X. H.; Liu, S. Q. *Anal. Chem.* **2011**, *83*, 6800−6809.
(7) Wang, S. J.; Harris, E.; Shi, J.; Chen, A.; Parajuli, S.; Jing, X. H.; Miao, W. J. *Phys. Chem. Chem. Phys.* **2010**, *12*, 10073−10080.
(8) Jie, G. F.; Wang, L.; Yuan, J. X.; Zhang, S. S. *Anal. Chem.* **2011**, *83*, 3873−3880.
(9) Chen, L. F.; Cai, Q. H.; Luo, F.; Chen, X.; Zhu, X.; Qiu, B.; Lin, Z. Y.; Chen, G. N. *Chem. Commun.* **2010**, *46*, 7751−7753.
(10) Tian, D. Y.; Duan, C. F.; Wang, W.; Cui, H. *Biosens. Bioelectron.* **2010**, *25*, 2290−2295.
(11) Jie, G. F.; Wang, L.; Zhang, S. S. *Chem.—Eur. J.* **2011**, *17*, 641−648.
(12) Wei, K. C.; Li, J.; Chen, G. S.; Jiang, M. *ACS Macro Lett.* **2013**, *2*, 278−283.
(13) Mirri, G.; Bull, S. D.; Horton, P. N.; James, T. D.; Male, L.; Tucker, J. H. R. *J. Am. Chem. Soc.* **2010**, *132*, 8903−8905.
(14) Krishnan, S.; Mani, V.; Wasalathanthri, D.; Kumar, C. V.; Rusling, J. F. *Angew. Chem., Int. Ed.* **2011**, *50*, 1175−1178.
(15) Pérez-Fuertes, Y.; Kelly, A. M.; Fossey, J. S.; Powell, M. E.; Bull, S. D.; James, T. D. *Nat. Protoc.* **2008**, *3*, 210−214.
(16) Kong, B.; Zhu, A. W.; Luo, Y. P.; Tian, Y.; Yu, Y. Y.; Shi, G. Y. *Angew. Chem., Int. Ed.* **2011**, *50*, 1837−1840.
(17) Metola, P.; Anslyn, E. V.; James, T. D.; Bull, S. D. *Chem. Sci.* **2012**, *3*, 156−161.
(18) Van Staden, J. F.; Van Staden, R. I. S. *Talanta* **2012**, *102*, 34−43.
(19) Ji, C. J.; Li, W. L.; Ren, X. D.; El-Kattan, A. F.; Kozak, R.; Fountain, S.; Lepsy, C. *Anal. Chem.* **2008**, *80*, 9195−9203.
(20) Abbaspour, A.; Khajehzadeh, A.; Ghaffarinejad, A. *Analyst* **2009**, *134*, 1692−1698.
(21) Ikeda, M.; Fukuda, K.; Tanida, T.; Yoshii, T.; Hamachi, I. *Chem. Commun.* **2012**, *48*, 2716−2718.
(22) Shang, N. G.; Papakonstantinou, P.; McMullan, M.; Chu, M.; Stamboulis, A.; Potenza, A.; Dhesi, S. S.; Marchetto, H. *Adv. Funct. Mater.* **2008**, *18*, 3506−3514.
(23) Zhang, Y.; Yuan, R.; Chai, Y. Q.; Li, W. J.; Zhong, X.; Zhong, H. A. *Biosens. Bioelectron.* **2011**, *26*, 3977−3980.
(24) Zhang, X.; Chen, C.; Li, J.; Zhang, L.; Wang, E. K. *Anal. Chem.* **2013**, *85*, 5335−5339.
(25) Liu, X.; Jiang, H.; Lei, J. P.; Ju, H. X. *Anal. Chem.* **2007**, *79*, 8055−8060.
(26) Cui, R.; Gu, Y. P.; Bao, L.; Zhao, J. Y.; Qi, B. P.; Zhang, Z. L.; Xie, Z. X.; Pang, D. W. *Anal. Chem.* **2012**, *84*, 8932−8935.
(27) Shi, C. G.; Shan, X.; Pan, Z. Q.; Xu, J. J.; Lu, C.; Bao, N.; Gu, H. Y. *Anal. Chem.* **2012**, *84*, 3033−3038.
(28) Li, Q.; Zheng, J. Y.; Yan, Y. L.; Zhao, Y. S.; Yao, J. N. *Adv. Mater.* **2012**, *24*, 4745−4749.
(29) Bao, L.; Sun, L. F.; Zhang, Z. L.; Jiang, P.; Wise, F. W.; Abruña, H. D.; Pang, D. W. *J. Phys. Chem. C* **2011**, *115*, 18822−18828.
(30) Ge, C. W.; Xu, M.; Liu, J.; Lei, J. P.; Ju, H. X. *Chem. Commun.* **2008**, *44*, 450−452.
(31) Deng, S. Y.; Lei, J. P.; Cheng, L. X.; Zhang, Y. Y.; Ju, H. X. *Biosens. Bioelectron.* **2011**, *26*, 4552−4558.
(32) Yu, W. W.; Qu, L. H.; Guo, W. Z.; Peng, X. G. *Chem. Mater.* **2003**, *15*, 2854−2860.
(33) Myung, N.; Bae, Y. J.; Bard, A. J. *Nano Lett.* **2003**, *3*, 1053−1055.
(34) Alivisatos, A. P. *Science* **1996**, *271*, 933−937.
(35) Zeng, Y.; Zhou, Y.; Kong, L.; Zhou, T.; Shi, G. *Biosens. Bioelectron.* **2013**, *45*, 25−33.
(36) Yu, C.; Luo, M.; Zeng, F.; Zheng, F.; Wu, S. *Chem. Commun.* **2011**, *47*, 9086−9088.
(37) Zen, J. M.; Hsu, C. T.; Hsu, Y. L.; Sue, J. W.; Conte, E. D. *Anal. Chem.* **2004**, *76*, 4251−4255.
(38) Zhang, M. N.; Liu, K.; Gong, K. P.; Su, L.; Chen, Y.; Mao, L. Q. *Anal. Chem.* **2005**, *77*, 6234−6242.
(39) Lin, Y. Q.; Zhang, Z. P.; Zhao, L. Z.; Wang, X.; Yu, P.; Su, L.; Mao, L. Q. *Biosens. Bioelectron.* **2010**, *25*, 1350−1355.
(40) Zhao, J. J.; Chen, M.; Yu, C. X.; Tu, Y. F. *Analyst* **2011**, *136*, 4070−4074.